Eur. J. Biochem. **263**, 264–269 (1999) © FEBS 1999

N-Tail translocation in a eukaryotic polytopic membrane protein

Synergy between neighboring transmembrane segments

Magnus Monné, Guro Gafvelin*, Robert Nilsson and Gunnar von Heijne

Department of Biochemistry, Stockholm University, Sweden

We have used the natural N-glycosylation site in the N-tail of cig30, a eukaryotic polytopic membrane protein, as a marker for N-tail translocation across the microsomal membrane. Analysis of C-terminally truncated cig30 constructs reveals that the first transmembrane segment is sufficient for translocation of the wild-type N-tail; in contrast, in a mutant with four arginines introduced into the N-tail the second transmembrane segment is also required for efficient N-tail translocation. Our observations imply a non-sequential assembly mechanism in which the ultimate location of the N-tail relative to the membrane may depend on more than one transmembrane segment.

Keywords: cig30; membrane protein assembly; N-tail translocation; topology.

Translocation of proteins across the membrane of the endoplasmic reticulum (ER) is normally initiated by an N-terminal signal peptide or signal-anchor sequence [1], resulting in translocation of the downstream part of the nascent chain. Many integral membrane proteins do not follow this simple N- to C-terminal translocation mechanism, however, but rather have their polar N-terminal tails (N-tails) translocated across the membrane into the lumen of the ER; this is the case for, e.g. most of the G-protein-coupled receptors [2]. For such proteins, the most N-terminal transmembrane (TM) segment is thought to function as a 'reverse signal-anchor sequence' [1] that targets the protein to the ER translocon via the normal signal recognition particle (SRP) pathway, but then inserts across the membrane with its N-terminal rather than C-terminal flanking domain facing the lumen. The net charge difference across the N-terminal TM [3], the length of this TM [4], and the folding properties of the N-tail domain [5] are all known to affect the efficiency of N-tail translocation.

According to the simplest model of how multispanning (polytopic) membrane proteins insert cotranslationally into the ER membrane [6], the hydrophobic TM segments serve alternately as start and stop transfer signals, and membrane insertion is thus viewed as a sequential process starting from the N-terminal TM. While this model, based on the notion of independently acting topogenic signals, may account for the assembly of some polytopic proteins, there are a number of counter examples where a given TM segment will only insert properly in the presence of its neighboring TMs but not otherwise [7–12], implying that topogenic information present in more than one TM must be 'decoded' simultaneously.

In this paper, we address the question of whether the most N-terminal TM in a polytopic eukaryotic protein, cig30 (cold-inducible glycoprotein of 30 kDa) [13], is by itself sufficient to induce translocation of the ≈35 residues long, lumenally oriented N-tail, or if additional topogenic information is needed. We find that the first TM is indeed the only hydrophobic segment that is required for efficient translocation of the N-tail, but that membrane targeting is inefficient unless TM1 is followed by a sufficiently long stretch of chain. In contrast, in a cig30 mutant in which additional positively charged residues have been inserted into the N-tail, efficient translocation is only observed when two transmembrane segments are present, and only if they are followed by a sufficiently long polar domain. These results indicate that topogenic information present in the entire N-tail–TM1–TM2 region can affect the topology of the protein, implying a non-sequential assembly mechanism in which the ultimate location of the N-tail may depend on more than one TM segment.

Correspondence to G. von Heijne, Department of Biochemistry, Stockholm University, S-106 91 Stockholm, Sweden. Fax: +46 8 15 36 79, Tel.: + 46 8 16 25 90, E-mail: gunnar@biokemi.su.se

Abbreviations: ER, endoplasmic reticulum; TM, transmembrane; SRP, signal recognition particle; cig30, cold-inducible 30-kDa glycoprotein.

**Present address:* Department of Laboratory Medicine, Division of Clinical Immunology, Karolinska Hospital, S-171 76 Stockholm, Sweden.

(Received 8 February 1999; revised 29 March 1999: accepted 22 April 1999)

MATERIALS AND METHODS

Enzymes and chemicals

Unless otherwise stated, all enzymes were from SDS Promega (Falkenberg, Sweden). Ribonucleotides, deoxyribonucleotides, dideoxyribonucleotides, the cap analog m7G(5′)-ppp(5′)G, T7 DNA polymerase, and [^{35}S]methionine were from Amersham-Pharmacia Biotech (Uppsala, Sweden). Plasmid pGEM1, dithiothreitol, BSA, RNasine, rabbit reticulocyte lysate, and the RiboMAX^{TM} system were from SDS Promega. Spermidine and phenylmethanesulfonyl fluoride were from Sigma. Oligonucleotides were from Cybergene (Stockholm, Sweden). Proteinase K was from Life Technologies, Inc.

DNA techniques

*Sal*I and *Xba*I restriction sites were introduced by PCR at the 5′ and 3′ ends of the *cig30* gene, respectively. The PCR fragment was cloned into phage M13 mp18 and into a pGEM1-derived plasmid after a modified upstream region of the *lepB* gene [14] containing a 'Kozak consensus sequence' for efficient ribosome binding [15]. Site-directed mutagenesis was performed as described by Kunkel and Geissloder [16,17] to introduce 4 arginine codons after the 9th or 28th codon in the cig30 coding

region, as well as to replace the acceptor asparagine in the N-glycosylation site at codon 6 with a serine. Fusion protein constructs were made by introducing an *Nde*I site in codon 70 (i.e. after TM1) or in codon 100 (i.e. after TM2) by PCR amplification using primers encoding the two flanking restriction sites. The *Sal*I–*Nde*I restricted PCR fragments were cloned into a pGEM1-derived vector containing the P2 domain (codon 81–323) of *Escherichia coli* protein leader peptidase (Lep) preceded by an *Nde*I site. Two versions of P2, with and without a consensus glycosylation site (NST) and both with an Asn214→Gln mutation, were used. Constructs were transformed into *E. coli* MC1061 by heat-shock treatment of Ca^{2+}-competent cells. All constructs were confirmed by sequencing of plasmid or single-stranded M13 DNA using T7 DNA polymerase. PCR was also used to amplify truncated parts of the *cig30* and 4R-9 mutant genes for *in vitro* translation. In this case, the 5′ primer was situated 210 bases upstream of the SP6 promoter in pGEM1, and the 3′ primers were designed with a stop codon at the required site.

Expression *in vitro*

The constructs in pGEM1 were transcribed by SP6 RNA polymerase for 1 h at 37 °C in a transcription mixture composed of 1–5 μg DNA template, 5 μL 10 × SP6 H-buffer (400 mM Hepes/KOH, pH 7.4, 60 mM magnesium acetate, 20 mM spermidine hydrochloride), 5 μL BSA (1 mg·mL^{-1}), 5 μL m7G(5′)ppp(5′)G (10 mM), 5 μL dithiothreitol (50 mM), 5 μL γNTP mix (10 mM ATP, 10 mM CTP, 10 mM UTP, 5 mM GTP), 18.5 μL water, 1.5 μL RNase inhibitor (50 units) and 0.5 μL SP6 RNA polymerase (20 units). The truncated PCR products of the *cig30* gene and the 4R-9 mutant were transcribed using the RiboMAX^{TM} system and SP6 RNA polymerase at 30 °C overnight. Translation was performed in reticulocyte lysate in the presence and absence of dog pancreas microsomes [18]. For carbonate extraction, 5 μL of the translation mixture was added to 90 μL Na_2CO_3 (0.1 M) and loaded on a 50-μL sucrose cushion (0.1 M Na_2CO_3 and 0.2 M sucrose) for centrifugation at 245 000 ***g*** for 10 min at 4 °C. The

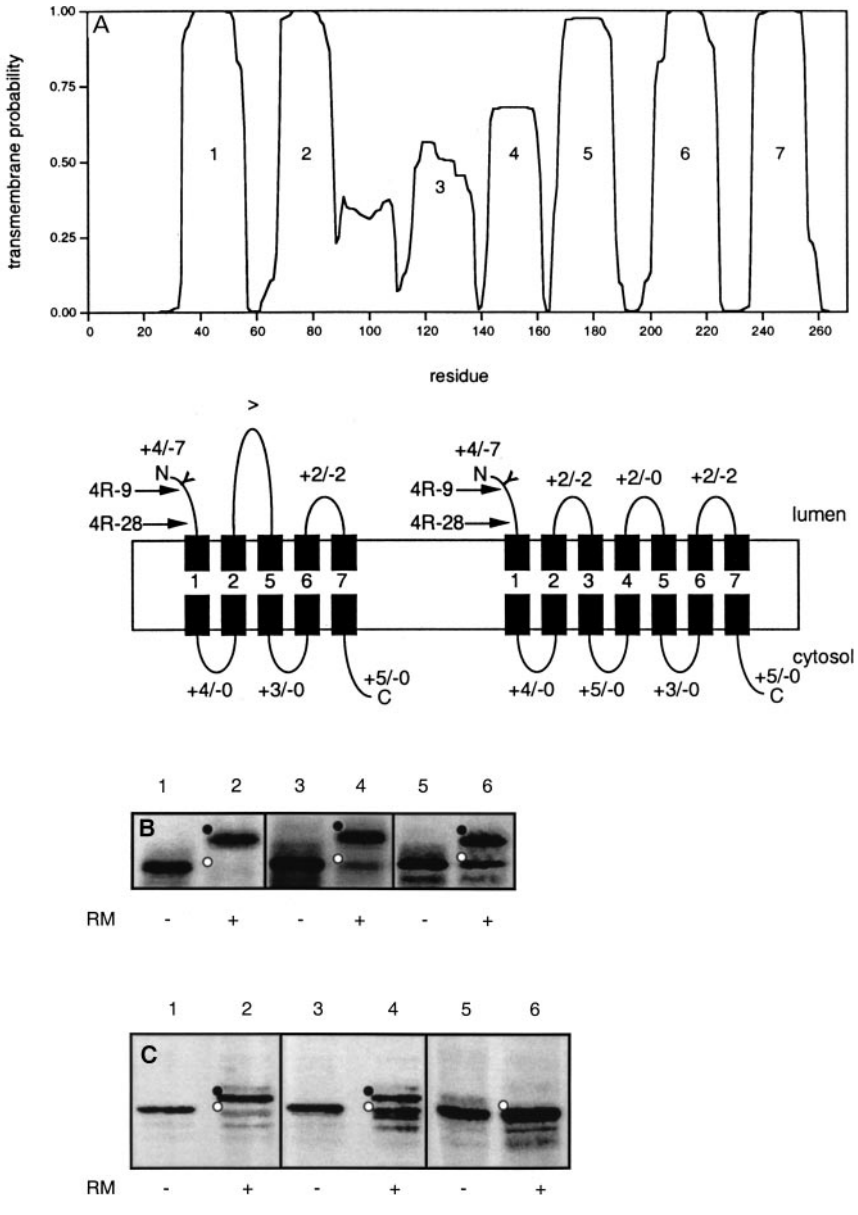

Fig. 1. Reduction of N-tail translocation in the 4R- mutants compared with wild-type cig30. (A) TMHMM [22] transmembrane segment prediction and putative 5TM and 7TM topologies of cig30. The number of positively (Lys + Arg) and negatively (Asp + Glu) charged residues in each loop is shown (the loop indicated by > is too long for the 'positive inside' rule to apply [20,33]). Arrows indicate where four consecutive arginines were introduced and Y indicates the N-glycosylation site at Asn6. (B) *In vitro* translation in rabbit reticulocyte lysate in the presence (+) and absence (–) of dog pancreas rough microsomes (RM). Lanes 1 and 2, wild-type cig30; lanes 3 and 4, 4R-28; lanes 5 and 6, 4R-9. (C) Full-length cig30/P2* (lanes 1, 2), 4R-9/P2* (lanes 3, 4), and cig30(Ser6)/P2* (lanes 5, 6) fusions were analyzed by *in vitro* translation as in (B). Glycosylated products are indicated by a black dot, and unglycosylated products by a white dot in (B) and (C).

translation products were analyzed by SDS/PAGE. The protein bands were quantified on a FUJIX BAS1000 phosphoimager using the MACBAS v2.31 software, and the glycosylation efficiency was calculated as the quotient between the intensity of the glycosylated band divided by the summed intensities of the glycosylated and non-glycosylated bands. In general, the glycosylation efficiency varied by no more than ± 5% between different experiments (two to five independent measurements were made for all constructs), except for the data presented in Fig. 2B, lanes 1–5, where the small size of the proteins made accurate quantitation somewhat more difficult. Translocation of polypeptide segments of the cig30/P2 fusions to the lumenal side of the microsomes was also assayed by resistance to exogenously added proteinase K [19].

Topology prediction

Prediction of the membrane topology of cig30 was carried out using TOPPRED II [20], DAS [21] and TMHMM [22].

RESULTS

Positively charged residues reduce N-tail translocation in full-length cig30

Cig30 is a polytopic membrane protein expressed in brown adipose tissue in mice, where it is involved in thermogenesis [13]. The protein has between five and seven predicted TM segments (Fig. 1A). A single N-glycosylation site in the ≈35-residue-long N-tail is efficiently modified with a high mannose oligosaccharide both *in vivo* and when the protein is expressed *in vitro* in the presence of dog pancreas microsomes [13], demonstrating that the N-tail is translocated into the lumen of the ER. No other potential N-glycosylation site is present in the sequence, and, on replacement of the acceptor asparagine (Asn6) with a serine, no modification was detected when the mutant protein was expressed in the presence of microsomes (data not shown).

In *E. coli* inner-membrane proteins, translocated N-tails generally contain few positively charged residues, and it has been shown that the introduction of extra basic residues efficiently blocks N-tail translocation [23–25]. Similarly, translocated N-tails in eukaryotic G-protein-coupled receptors have a reduced content of positively charged residues [2]. To test if the addition of arginines to N-tails is also detrimental to translocation in eukaryotic polytopic proteins, four consecutive arginine residues were inserted into the cig30 N-tail, either 9 or 28 residues away from the N-terminus (Fig. 1A). Wild-type cig30 as well as the 4R-9 and 4R-28 mutants were expressed *in vitro* in the absence and presence of dog pancreas microsomes, and the efficiency of glycosylation was taken as an indication of the extent of N-tail translocation. In this system, the maximal level of glycosylation seen for fully translocated proteins is generally 70–80%. As seen in Fig. 1B, the N-tail was very efficiently translocated in the wild-type protein (74% glycosylation), while the level of glycosylation was somewhat reduced in the 4R-28 and 4R-9 mutants (69% and 53% glycosylation, respectively). These values did not change when the membranes were carbonate-extracted to remove non-integrated molecules before the SDS/PAGE analysis (data not shown), demonstrating that membrane targeting was not affected by the 4R mutations. Thus, while there is an apparent effect on N-tail translocation in the 4R mutants, this is much less pronounced than that previously observed for the *E. coli* inner-membrane protein ProW, in which the addition of a single lysine (or two arginines) was enough to completely block translocation [24].

To check whether the introduced arginines cause an inverted topology of the whole protein, the large globular P2* domain (the asterisk indicates the presence of a potential N-glycosylation site at position 96) from the *E. coli* protein leader peptidase (Lep) was fused to the full-length forms of the cig30 protein and the 4R-9 mutant (Fig. 1C). No doubly glycosylated molecules were detected, and the levels of singly glycosylated molecules (71% for cig30/P2*, lane 2, and 45% for 4R-9/P2*, lane 4) were similar to those of the original full-length molecules, consistent with a cytosolic location of the P2* domain and thus an odd number of transmembrane segments in the whole cig30 molecule. As a control, the glycosylation site in the N-tail of cig30/P2* was removed by an Asn6→Ser mutation; in this case, no glycosylation was seen (Fig. 1C, lane 6). Thus, the addition of four arginines to the N-tail does not cause an inverted topology of the whole molecule.

TM1 is sufficient to induce translocation of the wild-type N-tail

To study the role of individual TM segments for N-tail translocation, we created truncated molecules by introducing stop codons in two positions in the coding region (Fig. 2A). A truncation mutant [cig30(1–70)] encompassing residues 1–70, i.e. with only 15 residues left downstream of TM1, was poorly glycosylated (Fig. 2B, (lane 2). However, a much higher fraction of the material remaining in the membrane pellet after carbonate extraction to remove non-integral membrane proteins [26] was glycosylated (≈65%, lane 3), suggesting that membrane targeting rather than N-tail translocation is affected

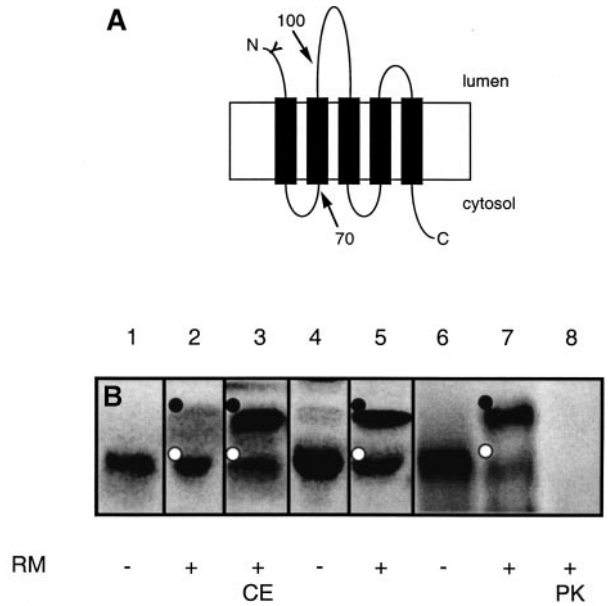

Fig. 2. TM1 directs the translocation of the cig30 N-tail if followed by a sufficiently long spacer sequence. (A) Truncations of cig30 were made by introducing stop codons at the positions indicated. In addition, cig30(1–70) was fused to the P2 domain of Lep. **Y** indicates the N-glycosylation site at Asn6. (B) Truncated transcripts were translated in the presence (+) and absence (–) of microsomes (RM). CE = carbonate-extracted membranes; PK = proteinase K-treated membranes. Lanes 1–3, cig30(1–70); lanes 4–5, cig30(1–100); lanes 6–8, cig30(1–70)/P2. Glycosylated products are indicated by a black dot and unglycosylated products by a white dot.

in this case. A longer construct, cig30(1–100), containing both TM1 and TM2 was fully glycosylated (≈70%), both before (lane 5) and after (data not shown) carbonate extraction.

To check whether the increase in targeting efficiency for cig30(1–100) was dependent on TM2 or simply a result of the increase in length, the P2 domain from Lep (the lack of an asterisk indicates the absence of an N-glycosylation site in P2) was fused downstream of TM1; indeed, the cig30(1–70)/P2 construct was efficiently targeted as seen by the high level of glycosylation even without carbonate extraction (63%; lane 7). Exogenously added proteinase K further verified the topology of the cig30(1–70)/P2 mutant, as no protease-protected fragment corresponding to a lumenally disposed P2 domain was seen after protease treatment of the microsomes (lane 8). Apparently, the cig30 N-tail can only be efficiently targeted if TM1 is followed by a sufficiently long stretch of chain, but this downstream domain does not have to include any additional TM segments.

TM1 + TM2 are required for efficient N-tail translocation of the 4R-9 mutant

While efficient translocation of the wild-type cig30 N-tail thus requires only TM1 and an additional downstream spacer region, we considered the possibility that TM1 alone might not suffice for the translocation of the 4R N-tail mutants. Initially, two P2 fusions were made in position 70 after TM1 for both the 4R-28

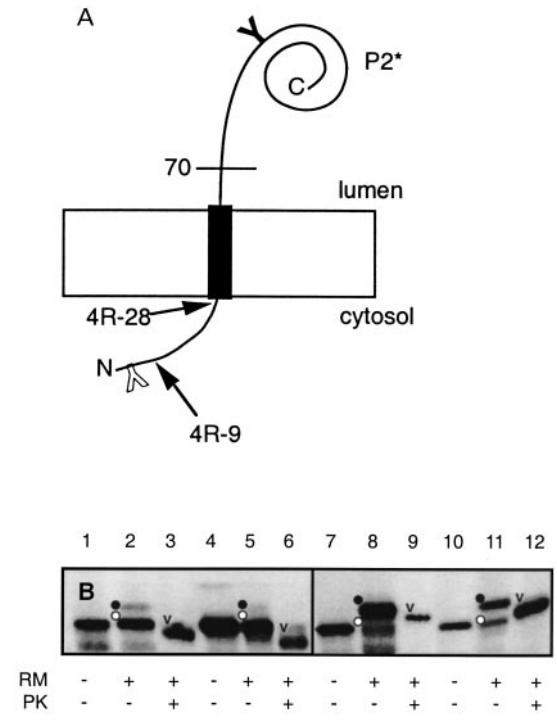

Fig. 3. TM1 is not sufficient for N-tail translocation in the 4R- mutants. (A) 4R-28(1–70) and 4R-9(1–70) were fused to the P2 (no glycosylation site) and P2* (glycosylation site in position 96) domains. **Y** and 𝕐 indicate modified and unmodified N-glycosylation sites, respectively. (B) Constructs were expressed in the presence (+) and absence (–) of microsomes (RM) and proteinase K (PK). The predominating topology is shown in (A). Lanes 1–3, 4R-28(1–70)/P2; lanes 4–6, 4R-9(1–70)/P2; lanes 7–9, 4R-28(1–70)/P2*; lanes 10–12, 4R-9(1–70)/P2*. Glycosylated products are indicated by a black dot and unglycosylated products by a white dot. Proteinase K-protected P2 and P2* domains are indicated by **v**.

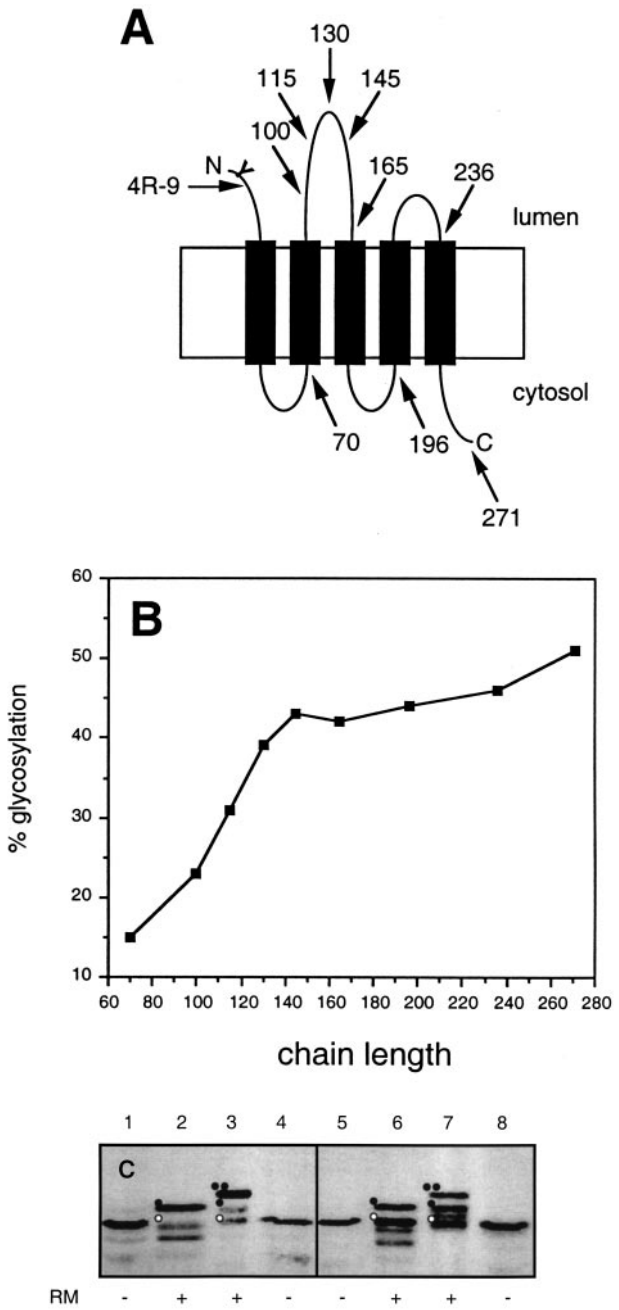

Fig. 4. Both TM1 and TM2 are required for translocation of the N-tail in the 4R-9 mutant. (A) Truncations of the 4R-9 mutant were made by introducing stop-codons at the positions indicated. (B) Truncated PCR products of the 4R-9 construct were transcribed *in vitro* and translated in the presence of microsomes. Translation products were subjected to carbonate extraction and ultracentrifugation over a sucrose cushion, and the membrane fractions were analyzed by SDS/PAGE. The glycosylation efficiency was quantified and plotted against the chain length. (C) cig30(1–100)/P2,P2* and 4R-9(1–100)/P2,P2* constructs were expressed in the presence (+) and absence (–) of microsomes (RM). Lanes 1 and 2, cig30(1–100)/P2; lanes 3 and 4, cig30(1–100)/P2*; lanes 5 and 6, 4R-9(1–100)/P2; lanes 7 and 8, 4R-9(1–100)/P2*. Doubly glycosylated products are indicated by two black dots, singly glycosylated products by one black dot, and unglycosylated products by a white dot.

and 4R-9 mutants, one carrying a glycosylation acceptor site in the P2 domain [mutants 4R-28(1–70)/P2* and 4R-9(1–70)/P2*] and one lacking such a site [mutants 4R-28(1–70)/P2 and 4R-9(1–70)/P2] (Fig. 3A). As seen in Fig. 3B, both constructs lacking a glycosylation site in the P2 domain were poorly glycosylated on their N-tails (lanes 2 and 5), while the constructs with glycosylation sites in both the N-tail and the P2 domain were efficiently glycosylated (lanes 8 and 11). Further, all constructs gave rise to proteinase K-protected fragments of sizes expected for the unglycosylated P2 and glycosylated P2* domains, respectively (lanes 3, 6, 9, 12). Thus, for both fusions an inverted topology with a cytosolic N-tail and a lumenal P2 domain predominate. The presence of the extra positively charged residues in the N-tail is apparently sufficient to largely prevent N-tail translocation and induce the N-tail-TM1/P2 fusion proteins to adopt an N_{cyt}-C_{lum} orientation.

As N-tail translocation was considerably more efficient in the full-length 4R-28 and 4R-9 mutants (Fig. 1B) than in the 4R-28(1–70)/P2 and 4R-9(1–70)/P2 fusion constructs (Fig. 3B), we made a series of successively longer truncated versions of the 4R-9 mutant in order to determine how much of the protein was needed for N-tail translocation to reach the level seen for the full-length protein (Fig. 4A). In contrast with cig30(1–70) after carbonate extraction (Fig. 2B), the membrane-integrated material from the shortest 4R-9-derived deletion mutants was poorly glycosylated, and a level of glycosylation approaching that seen for the full-length 4R-9 mutant was only reached for chains longer than ≈145 residues (Fig. 4B). In the 4R-9(1–145) construct, there are about 55 residues between the end of TM2 and the stop codon, suggesting that TM2 must be fully exposed outside the ribosome – which covers some 40 residues of the nascent chain [27,28] – in order for the N-tail to be as efficiently translocated as in the full-length 4R-9 mutant.

To verify the orientation of TM2 further and to ascertain that the increased translocation efficiency for the 4R-9(1–145) construct was independent of the specific sequence of the segment following TM2, fusions with the P2 domain with (P2*) and without (P2) a glycosylation site were made in position 100, ≈10 residues downstream of TM2 (Fig. 4C). 4R-9(1–100)/P2 was glycosylated (42%, lane 6) to the same extent as 4R-9(1–145) (43%, Fig. 4B), indicating that translocation of the N-tail is independent of the sequence of the segment following TM2. 4R-9(1–100)/P2* gave rise to three forms (32% glycosylated twice, 34% glycosylated once, and 34% not at all; lane 7); after treatment with proteinase K, these fractions did not change significantly (data not shown). Taken together, these data suggest that, while the P2-domain is efficiently translocated, only about half of the 4R-9(1–100)/P2 molecules have their N-tails translocated. There is no indication of non-glycosylated molecules with an inverted N_{cyt}-C_{cyt} topology, as such molecules would be degraded by proteinase K, shifting the relative amounts of glycosylated and non-glycosylated molecules after protease treatment. For comparison, cig30(1–100)/P2 and cig30(1–100)/P2* constructs were made; in both cases, efficient glycosylation of both the N-tail and P2 domain was seen (Fig. 4C, lanes 2 and 3), confirming the expected N_{lum}-C_{lum} topology.

DISCUSSION

The translocation of N-tails of polytopic membrane proteins across the ER membrane is a poorly understood process. Although it is known that the presence of positively charged residues in, and rapid folding of, the N-tail prevents its translocation [3,5], the effect of the downstream hydrophobic segment(s) has not been studied in detail.

cig30 is a polytopic membrane protein expressed in brown adipose tissue [13]. Although the topology of cig30 is not fully known, the efficient modification of the natural glycosylation site in the N-tail as well as the analysis of cig30/P2 fusions after putative TM1, TM2, and at the C-terminus (Figs 1, 2, and 4) are consistent with either a 5TM or 7TM topology. Here, we show that the N-terminal TM1 can induce efficient N-tail translocation, but that membrane targeting is compromised unless TM1 is followed by a sufficiently long downstream segment. A C-terminal tail of ≈45 residues allows efficient targeting and N-tail translocation (Fig. 2), suggesting that TM1 must be exposed outside the ribosome before termination of translation, i.e. that SRP binding and membrane targeting must be cotranslational. In wild-type cig30, TM1 thus appears to be sufficient for N-tail translocation.

In contrast, N-tail translocation in a mutant with four extra arginines in the N-tail (mutant 4R-9) can only be restored to the level seen for the full-length protein if both TM1 and TM2 are present, and if in addition the C-tail downstream of TM2 is at least 55 residues long (Figs 3 and 4). Thus, when the N-tail is intrinsically difficult to translocate, TM1 alone is not sufficient to impart the topology seen for the full-length protein. The finding that TM2 needs to be followed by a C-terminal tail of ≈55 residues or more for full N-tail translocation indicates that TM2 must be able to interact with SRP while the nascent chain is still attached to the ribosome; possibly TM2 can then compete efficiently with TM1 for binding to SRP, which might promote its subsequent membrane insertion with the normal N_{cyt}-C_{lum} orientation. With TM2 already inserted in this orientation, TM1 has no choice but to insert with an N_{lum}-C_{cyt} orientation, thus carrying the N-tail to the lumenal side. There are no obvious sequence characteristics (e.g. overall hydrophobicity) that might cause TM2 to bind more tightly to SRP than TM1, but we note that previous studies of tandem signal peptides have indicated that the downstream signal tends to dominate the upstream signal when they are not too far apart [29,30].

Whether the somewhat inefficient glycosylation of the N-tail in the full-length 4R-9 mutant results only from inefficient translocation (leaving the N-tail/TM1 region on the cytosolic side) in a fraction of the molecules or if the four arginines may also affect the efficiency with which the glycosylation site -Met-Asn6-Phe-Ser-Arg- is modifed by the oligosaccharyl transferase is difficult to determine. Studies on a model protein suggest that downstream arginines provide a favorable context for glycosylation of Asn-X-Ser acceptor sites [31]. In any case, this does not affect the conclusions on the role of TM2 for N-tail translocation in the 4R-9 mutant.

In summary, our results suggest that efficient N-tail translocation in polytopic eukaryotic membrane proteins may, at least in certain situations, depend on more than one TM segment and on whether the critical topogenic segment(s) are presented outside the ribosome co- or post-translationally, a finding that is incompatible with a simple sequential N- to C-terminal insertion process. As the net charge difference across the N-terminal TM is the same in all the 4R-9 constructs, it is obvious that the final topology adopted by the protein is not only determined by the so-called 'net-charge' rule [32].

ACKNOWLEDGEMENTS

A plasmid containing the cDNA of *cig30* gene was kindly provided by Anders Jacobsson, Department of Metabolic Research, Stockholm

University. This work was supported by grants from the Swedish Natural and Technical Sciences Research Councils, the Swedish Cancer Foundation, and the Göran Gustafsson Foundation to GvH.

REFERENCES

1. von Heijne, G. (1988) Transcending the impenetrable: how proteins come to terms with membranes. *Biochim. Biophys. Acta* **947**, 307–333.
2. Wallin, E. & Heijne, G. (1995) Properties of N-terminal tails in G-protein coupled receptors: a statistical study. *Protein Eng.* **8**, 693–698.
3. Wahlberg, J.M. & Spiess, M. (1997) Multiple determinants direct the orientation of signal-anchor proteins: the topogenic role of the hydrophobic signal domain. *J. Cell Biol.* **137**, 555–562.
4. Sakaguchi, M., Tomiyoshi, R., Kuroiwa, T., Mihara, K. & Omura, T. (1992) Functions of signal and signal-anchor sequences are determined by the balance between the hydrophobic segment and the N-terminal charge. *Proc. Natl Acad. Sci. USA* **89**, 16–19.
5. Denzer, A.J., Nabholz, C.E. & Spiess, M. (1995) Transmembrane orientation of signal-anchor proteins is affected by the folding state but not the size of the N- terminal domain. *EMBO J.* **14**, 6311–6317.
6. Blobel, G. (1980) Intracellular protein topogenesis. *Proc. Natl Acad. Sci. USA* **77**, 1496–1500.
7. Gafvelin, G., Sakaguchi, M., von Andersson, H. & Heijne, G. (1997) Topological rules for membrane protein assembly in eukaryotic cells. *J. Biol. Chem* **272**, 6119–6127.
8. Skach, W.R., Calayg, M.C. & Lingappa, V.R. (1993) Evidence for an alternate model of human P-glycoprotein structure and biogenesis. *J. Biol. Chem* **268**, 6903–6908.
9. Lu, Y., Xiong, X.M., Helm, A., Kimani, K., Bragin, A. & Skach, W.R. (1998) Co- and posttranslational translocation mechanisms direct cystic fibrosis transmembrane conductance regulator N terminus transmembrane assembly. *J. Biol. Chem.* **273**, 568–576.
10. Zhang, J.T., Lee, C.H., Duthie, M. & Ling, V. (1995) Topological determinants of internal transmembrane segments in P-glycoprotein sequences. *J. Biol. Chem.* **270**, 1742–1746.
11. Chen, M. & Zhang, J.-T. (1996) Membrane insertion, processing, and topology of cystic fibrosis transmembrane conductance regulator (CFTR) in microsomal membranes. *Mol Membr. Biol.* **13**, 33–40.
12. Ota, K., von Sakaguchi, M., Heijne, G., Hamasaki, N. & Mihara, K. (1998) Forced transmembrane orientation of hydrophilic polypeptide segments in multispanning membrane proteins. *Mol. Cell* **2**, 495–503.
13. Tvrdik, P., Asadi, A., Kozak, L., Nedergaard, J., Cannon, B. & Jacobsson, A. (1997) Cig30, a mouse member of a novel membrane protein gene family, is involved in the recruitment of brown adipose tissue. *J. Biol. Chem.* **272**, 31738–31746.
14. Johansson, M., von Nilsson, I. & Heijne, G. (1993) Positively charged amino acids placed next to a signal sequence block protein translocation more efficiently in *Escherichia coli* than in mammalian microsomes. *Mol. Gen. Genet.* **239**, 251–256.
15. Kozak, M. (1989) Context effects and inefficient initiation at non-AUG codons in eucaryotic cell-free translation systems. *Mol. Cell Biol.* **9**, 5073–5080.
16. Geisselsoder, J., Witney, F. & Yuckenberg, P. (1987) Efficient site-directed *in vitro* mutagenesis. *Biotechniques* **5**, 786–791.
17. Kunkel, T.A. (1985) Rapid and efficient site-specific mutagenesis without phenotypic selection. *Proc. Natl Acad. Sci. USA* **82**, 488–492.
18. Liljeström, P. & Garoff, H. (1991) Internally located cleavable signal sequences direct the formation of Semliki Forest virus membrane proteins from a polyprotein precursor. *J. Virol.* **65**, 147–154.
19. Nilsson, I. & Heijne, G. (1993) Determination of the distance between the oligosaccharyltransferase active site and the endoplasmic reticulum membrane. *J. Biol. Chem.* **268**, 5798–5801.
20. Claros, M.G. & Heijne, G. (1994) TopPred II: an improved software for membrane protein structure prediction. *Comput. Appl. Biosci.* **10**, 685–686.
21. Cserzö, M., Wallin, E., von Simon, I., Heijne, G. & Elofsson, A. (1997) Prediction of transmembrane α-helices in prokaryotic membrane proteins: the Dense Alignment Surface method. *Protein Eng.* **10**, 673–676.
22. Sonnhammer, E., Heijne, G. & Krogh, A. (1998) A hidden Markov model for predicting transmembrane helices in protein sequences. *Intell. Syst. Mol. Biol.* **6**, 175–182.
23. Whitley, P., Zander, T., Ehrmann, M., Haardt, M., von Bremer, E. & Heijne, G. (1994) *Sec*-independent translocation of a 100-residues long periplasmic N-terminal tail in the *E. coli* inner membrane proteins ProW. *EMBO J.* **13**, 4653–4661.
24. Whitley, P., von Gafvelin, G. & Heijne, G. (1995) *Sec*-independent translocation of the periplasmic N-terminal tail of an *E. coli* inner membrane protein: position-specific effects on translocation of positively charged residues and construction of a protein with a C-terminal translocation signal. *J. Biol. Chem.* **270**, 29831–29835.
25. Cao, G.Q. & Dalbey, R.E. (1994) Translocation of N-terminal tails across the plasma membrane. *EMBO J.* **13**, 4662–4669.
26. Fujiki, Y., Hubbard, A.L., Fowler, S. & Lazarow, P.B. (1982) Isolation of intracellular membranes by means of sodium carbonate treatment. *J. Cell Biol.* **93**, 97–102.
27. Malkin, L. & Rich, A. (1967) Partial resistance of nascent polypeptide chains to proteolytic digestion due to ribosomal shielding. *J. Mol. Biol.* **26**, 329–346.
28. Blobel, G. & Sabatini, D.D. (1970) Controlled proteolysis of nascent polypeptides in rat liver cell fractions. I. Location of the polypeptides within ribosomes. *J. Cell Biol.* **45**, 130–145.
29. Coleman, J., Inukai, M. & Inouye, M. (1985) Dual functions of the signal peptide in protein transfer across the membrane. *Cell* **43**, 351–360.
30. Chen, H.F., Kim, J. & Kendall, D.A. (1996) Competition between functional signal peptides demonstrates variation in affinity for the secretion pathway. *J. Bacteriol.* **178**, 6658–6664.
31. Mellquist, J.L., Kasturi, L., Spitalnik, S.L. & Shakin-Eshleman, S.H. (1998) The amino acid following an Asn-X-Ser/Thr sequon is an important determinant of N-linked core glycosylation efficiency. *Biochemistry* **37**, 6833–6837.
32. Hartmann, E., Rapoport, T.A. & Lodish, H.F. (1989) Predicting the orientation of eukaryotic membrane proteins. *Proc. Natl Acad. Sci. USA* **86**, 5786–57890.
33. Sipos, L. & Heijne, G. (1993) Predicting the topology of eukaryotic membrane proteins. *Eur. J. Biochem.* **213**, 1333–1340.